



CHORUS

This is the accepted manuscript made available via CHORUS. The article has been published as:

Equivalent expression of Z_2 topological invariant for band insulators using the non-Abelian Berry connection

Rui Yu, Xiao Liang Qi, Andrei Bernevig, Zhong Fang, and Xi Dai

Phys. Rev. B **84**, 075119 — Published 8 August 2011

DOI: [10.1103/PhysRevB.84.075119](https://doi.org/10.1103/PhysRevB.84.075119)

An equivalent expression of Z_2 Topological Invariant for band insulators using Non-Abelian Berry's connection

Rui Yu¹, Xiao Liang Qi², Andrei Bernevig³, Zhong Fang¹ and Xi Dai¹

¹*Beijing National Laboratory for Condensed Matter Physics and Institute of Physics, Chinese Academy of Sciences, Beijing 100080, China*

²*Department of Physics, Stanford University, Stanford, California 94305, USA and*

³*Department of Physics, Princeton University, Princeton, New Jersey 08540, USA*

(Dated: June 2, 2011)

We introduce a new expression for the Z_2 topological invariant of band insulators using non-Abelian Berry's connection. Our expression can identify the topological nature of a general band insulator *without* any of the gauge fixing problems that plague the concrete implementation of previous invariants. The new expression can be derived from the "partner switching" of the Wannier function center during time reversal pumping and is thus equivalent to the Z_2 topological invariant proposed by Kane and Mele. Using the new expression, we have recalculated the Z_2 topological index for several topological insulator material systems and obtained consistent results with the previous studies.

PACS numbers: 71.15.-m, 71.27.+a, 71.15.Mb

I. INTRODUCTION

Topological invariants play a very important role in the classification of band insulators. The studies on integer quantum Hall effect (IQHE) show that 2D band insulators without time reversal symmetry can be classified by the Chern number - an integer describing the topological structure of a set of fully occupied Bloch bands without Kramers degeneracy. Systems with non-zero Chern number exhibit IQHE^{1,2}.

A similar idea can be also applied to band insulators with time reversal symmetry. A Z_2 topological invariant has been proposed by Kane and Mele to characterize the time reversal invariant band insulators in 2D^{3,4}. According to this new topological invariant, all the 2D band insulators with time-reversal invariance can be divided into two classes. The normal insulators with even Z_2 number and topological insulators with odd Z_2 number⁵⁻⁷. The 2D topological insulators will exhibit a quantum spin Hall effect (QSHE)^{3,8}, which is characterized by the presence of helical edge states^{3,8-14}. Interestingly the Z_2 topological invariant can also be generalized to the 3D band insulators with time reversal symmetry^{5,6,15}. In this case, there are four independent Z_2 topological numbers: one strong topological index and three weak topological indices¹⁵⁻¹⁹. The 3D time reversal invariant band insulators can be classified as normal insulators, weak topological insulators (WTI) and strong topological insulators (STI) according to the values of these four Z_2 topological indices. Among them, the STI attracts much attention due to its unique Dirac type surface states and robustness against disorder²⁰⁻³¹. The helical spin structure of the Dirac type surface states has been experimentally verified by the standing wave structure in scanning tunneling microscope (STM) images around an impurity scattering center and measured directly by spin resolved angle resolved photo emission spectra (ARPES)³²⁻⁴⁰. The Dirac type 2D electron gas living on the surface of STI or at the

interface between STI and normal insulators provides a new playground for spintronics and quantum computing.

Since the Z_2 invariant characterizes whether a system is topologically trivial or nontrivial, its computation is essential to the field of topological insulators. For band insulators with extra spacial inversion symmetry, the Z_2 topological numbers can be easily computed as the product of half of the parity (Kramers pairs have identical parities) numbers for all the occupied states at the high symmetry points¹⁶. The situation becomes complicated in the general case where spacial inversion symmetry is absent. At the present, numerically there are three different ways to judge whether a band insulator without inversion symmetry is a topological insulator or not. i) Compute the Z_2 numbers using the integration of both Berry's connection and curvature over half of the Brillouin Zone (BZ). In order to do so, one has to set up a mesh in the k-space and calculate the corresponding quantities on the lattice version of the problem^{18,41,42}. Since the calculation involves the Berry's connection, one has to numerically fix the gauge on the half BZ, which is not easy for the realistic wave functions obtained by first principle calculation. ii) Start from an artificial system with spacial inversion symmetry, and then smoothly "deform" the Hamiltonian towards the realistic one without inversion symmetry. If the energy gap never closes at any points in the BZ during the "deformation" process, the realistic system must share the same topological nature with the initial reference system whose Z_2 number can be easily counted by the inversion eigenvalue formula. Unfortunately making sure that the energy gap remains open on the whole BZ is very difficult numerically, especially in 3D. iii) Directly calculate the surface states. For most of the topological insulator materials, the first principle calculation for the surface states is numerically heavy. Therefore it is valuable to develop a mathematically equivalent way to calculate the Z_2 numbers of a band insulator, which satisfies the following conditions:

first it should use only the periodic bulk system; second, it should not require any gauge fixing condition - thereby greatly simplifying the calculation; third, it should be easily applied to general systems lacking spacial inversion symmetry.

In the present paper we propose a new equivalent expression for the Z_2 topological invariant using the $U(2N)$ non-Abelian Berry connection. Based on this new expression, we further propose a new numerical method to calculate the Z_2 topological number for general band insulators, without choosing a gauge fixing condition. The main idea of the method is to calculate the evolution of the Wannier function center directly during a "time reversal pumping" process, which is a Z_2 analog to the charge polarization^{43,44}. We derive that the center of the Wannier function for the effective 1D system can be expressed as the $U(1)$ phase of the eigenvalues of a matrix obtained as the product of the $U(2N)$ Berry connection along the "Wilson loop". The Z_2 topological numbers can be expressed as the number of times mod 2 of the partner switching of these phases during a complete period of the "time reversal pumping" process. Using this new method, we have recalculated the Z_2 topological numbers for several topological insulator systems, including strained HgTe, Bi, Sb and Bi₂Se₃, and found the "partner switching" patterns, which differentiate between topologically trivial and nontrivial behavior. The rest of paper will be organized as follows: in section II we derive the new mathematical form of the Z_2 numbers through the "Wilson loop"; we apply the new method to various topological insulator systems in section III; we prove the equivalence of the new methods and the Z_2 number propose by Fu and Kane⁷ in the appendices.

II. THE FORMALISM

We assume that the Hamiltonian of a band insulator with both time reversal and translational symmetry can be expressed in terms of a complete set of local basis $\phi_\alpha(\mathbf{r} - \mathbf{R}_i)$, where \mathbf{R}_i denotes the position of the i 'th lattice site and α denotes the index of the local basis. We have

$$H = \sum_{\alpha\beta} \sum_{ij} h_{ij}^{\alpha\beta} |\alpha i\rangle \langle \beta j| + H.C. \quad (1)$$

where $h_{ij}^{\alpha\beta} = \int \phi_\alpha^*(\mathbf{r} - \mathbf{R}_i) H_{LDA}(\mathbf{r}) \phi_\beta(\mathbf{r} - \mathbf{R}_j) d\mathbf{r}^3$ with $H_{LDA}(\mathbf{r})$ being the Hamiltonian obtained by the first principle calculation, i.e. the local density approximation (LDA).

Therefore the Bloch eigen state of the above tight binding Hamiltonian, can be expressed as:

$$|\Psi_{n\mathbf{k}}\rangle = \sum_{\alpha} g_{n\alpha}(\mathbf{k}) |\alpha\mathbf{k}\rangle \quad (2)$$

$|\alpha\mathbf{k}\rangle = \frac{1}{\sqrt{N_{cell}}} \sum_i |\alpha i\rangle e^{i\mathbf{k}\cdot\mathbf{R}_i}$ is the Bloch sum of the corresponding local basis, n is the band index and $g_{n\alpha}(\mathbf{k})$ can be viewed as the wave function of the Bloch state in the momentum space. For convenience we denote the periodic part of the Bloch eigen state by $|n, \mathbf{k}\rangle$, where $|n, \mathbf{k}\rangle = e^{-i\mathbf{k}\cdot\mathbf{r}} |\Psi_{n\mathbf{k}}\rangle$, with \mathbf{r} the position operator.

We will first focus on the 2D system. The topological nature of a 3D insulator can later be determined by looking at these effective 2D systems with one of the momenta fixed at $k_i = 0$ and $k_i = \pi$ ($i = x, y, z$). In Ref.7 it was shown that the topological invariant in the 2D topological insulator can be described by an adiabatic pumping of "time-reversal polarization". Each wavevector k_y defines a one-dimensional subsystem, for which the time-reversal polarization is defined by splitting the bands in the system into two groups which are time-reversal partner of each other, and calculating the net charge polarization of one group of bands. The charge polarization is related to the position of Wannier functions in the subsystem, and the time-reversal polarization can be understood as the adiabatic shift of the Wannier functions. This calculation requires to make a global choice in splitting the occupied bands in the system into two groups, which may be difficult to do in general.

The main idea of our new formalism is to directly look at the evolution of Wannier function centers for these effective 1D systems of fixed k_y in the subspace of occupied states. Fixing k_y , maximally-localized Wannier functions (MLWF) in the one-dimensional subsystem can be obtained as eigenstates of the position operator projected into occupied subspace⁴⁵. For a 1D lattice system with periodic condition, the position operator is defined as

$$\hat{X} = \sum_{i\alpha} e^{-i\delta k_x \cdot \mathbf{R}_i} |\alpha i\rangle \langle \alpha i| \quad (3)$$

where $\delta k_x \equiv \frac{2\pi}{N_x a_x}$, N_x is the number of real-space unit cells along the x direction, a_x is the lattice constant, α is the orbital and spin index and \mathbf{R}_i labels the unit cell. We note that the periodic boundary condition is used here. In the limit of an infinite lattice $\delta k_x \rightarrow 0$ and we can instead define the Hermitian position operator $\hat{x} = \sum_{i\alpha} R_i |\alpha i\rangle \langle \alpha i| = i \frac{\partial}{\partial k_x}$, but it is more convenient for us to use the periodic boundary condition for the purpose of numerical calculation. The operator \hat{X} is a unitary operator with all the eigenvalues being $e^{-i\delta k_x \cdot \mathbf{R}_i}$, whose phase represents the position. The eigenvalue of the position operator can be viewed as the center of MLWF formed by the bands included in the operator \hat{X} .⁴⁵ Because the local basis set α is assumed to be complete, such MLWFs are always well defined. As pointed out by Fu and Kane, the Z_2 topological invariant can be determined by looking at the evolution of the Wannier function center for the effective 1D system with fixed k_y in the subspace spanned by the occupied bands only. The projection operator for the occupied subspace can be defined as

$$\hat{P}_{k_y} = \sum_{n \in o, k_x} |\Psi_{n\mathbf{k}}\rangle \langle \Psi_{n\mathbf{k}}| \quad (4)$$

where o in the summation means the occupied bands. Therefore we should consider the eigenvalue of the projected position operator defined as

$$\begin{aligned}
\hat{X}_P(k_y) &= \hat{P}_{k_y} \hat{X} \hat{P}_{k_y} \\
&= \sum_{nm \in o} \sum_{k_x k'_x, i\alpha} e^{-i\delta k_x \cdot \mathbf{R}_i} |\Psi_{nk_x, k_y}\rangle \langle \Psi_{nk_x, k_y}| \\
&\quad \times |\alpha i\rangle \langle \alpha i| \Psi_{mk'_x, k_y}\rangle \langle \Psi_{mk'_x, k_y}| \\
&= \sum_{nm \in o} \sum_{k_x k'_x, i} \frac{1}{N_{\text{cell}}} e^{i(k_x + \delta k_x - k'_x) \cdot \mathbf{R}_i} |\Psi_{nk_x, k_y}\rangle \langle \Psi_{mk'_x, k_y}| \\
&\quad \times \left[\sum_{\alpha} g_{n\alpha}^*(k_x) g_{m\alpha}(k'_x) \right] \\
&= \sum_{k_x k'_x} \delta(k_x + \delta k_x - k'_x) \sum_{nm \in o} |\Psi_{nk_x, k_y}\rangle \langle \Psi_{mk'_x, k_y}| \\
&\quad \times \left[\sum_{\alpha} g_{n\alpha}^*(k_x) g_{m\alpha}(k'_x) \right] \quad (5)
\end{aligned}$$

The above operator can be written in a more suggestive matrix form

$$\hat{X}_P(k_y) = \begin{bmatrix} 0 & F_{0,1} & 0 & 0 & 0 & 0 \\ 0 & 0 & F_{1,2} & 0 & 0 & 0 \\ 0 & 0 & 0 & F_{2,3} & 0 & 0 \\ 0 & 0 & 0 & 0 & \dots & 0 \\ 0 & 0 & 0 & 0 & 0 & F_{N_x-2, N_x-1} \\ F_{N_x-1, 0} & 0 & 0 & 0 & 0 & 0 \end{bmatrix} \quad (6)$$

where

$$F_{i, i+1}^{mn}(k_y) = \sum_{\alpha} g_{n\alpha}^*(k_{x,i}, k_y) g_{m\alpha}(k_{x, i+1}, k_y) \quad (7)$$

are the $2N \times 2N$ matrices spanned in $2N$ occupied states, $k_{x,i} = \frac{2\pi i}{N_x a_x}$ are the discrete k points taken along the x -axis.

In the following we will further prove that for a lattice Hamiltonian eq.(1), the above equation eq.(7) equals to the inner product of the periodic parts of the Bloch functions. We note that for a Hamiltonian defined on the lattice, the local bases $|\alpha i\rangle$ can be factorized into the "internal freedom" part and spacial part

$$|\alpha i\rangle = |\alpha\rangle \delta(\mathbf{r} - \mathbf{R}_i) \quad (8)$$

where α is the combined index for spin and orbital, $|\alpha\rangle = (0, 0, \dots, 1, \dots, 0, 0)^T$ is the basis vector with only α th component to be none zero. Under this definition we

have

$$\begin{aligned}
\langle n, k | m, k' \rangle &= \langle \Psi_{nk} | e^{ik \cdot r} e^{-ik' \cdot r} | \Psi_{m, k'} \rangle \\
&= \sum_{\alpha, \beta} \frac{1}{N_{\text{cell}}} g_{n\alpha}^*(k) g_{m\beta}(k') \\
&\quad * \sum_{j_1, j_2} \langle \alpha j_1 | e^{i(k-k') \cdot r} | \beta j_2 \rangle e^{i(k' \cdot R_{j_2} - k \cdot R_{j_1})} \\
&= \sum_{\alpha, \beta} \frac{1}{N_{\text{cell}}} g_{n\alpha}^*(k) g_{m\beta}(k') \\
&\quad * \sum_{j_1, j_2} \langle \alpha | \beta \rangle \delta_{j_1 j_2} e^{i(k-k') \cdot R_{j_2}} e^{i(k' \cdot R_{j_2} - k \cdot R_{j_1})} \\
&= \sum_{\alpha, \beta} g_{n\alpha}^*(k) g_{m\beta}(k') \delta_{\alpha\beta} \\
&= \sum_{\alpha} g_{n\alpha}^*(k) g_{m\alpha}(k') \quad (9)
\end{aligned}$$

and equivalently we have

$$F_{i, i+1}^{mn}(k_y) = \langle m, k_{x,i}, k_y | n, k_{x, i+1}, k_y \rangle \quad (10)$$

The eigen problem of $\hat{X}_P(k_y)$ can be solved by the transfer matrix method. We can define a product of $F_{i, i+1}$ as

$$D(k_y) = F_{0,1} F_{1,2} F_{2,3} \dots F_{N_x-2, N_x-1} F_{N_x-1, 0} \quad (11)$$

$D(k_y)$ is a $2N \times 2N$ matrix. which has $2N$ eigenvalues:

$$\lambda_m^D(k_y) = |\lambda_m^D| e^{i\theta_m^D(k_y)} \quad m = 1, 2, \dots, 2N$$

where $\theta_m^D(k_y)$ is the phase of the eigenvalues:

$$\theta_m^D(k_y) = \text{Im}(\log \lambda_m^D(k_y)) \quad (12)$$

The eigenvalues of $D(k_y)$ is gauge-invariant under a $U(2N)$ transformation of $|n, \mathbf{k}\rangle$. We can easily prove that the eigenvalue of projected position operator $\hat{X}_P(k_y)$ can be simply related to the eigenvalue of the above D -matrix by

$$\lambda_{m,n}^P = \sqrt[N_x]{\lambda_m^D} = \sqrt[N_x]{|\lambda_m^D|} e^{i(\theta_m^D + 2\pi n)/N_x} \quad (13)$$

where $n = 1, 2, \dots, N_x$. We can further prove that the D -matrix is unitary and all the $|\lambda_m^D|$ equals one.

For infinitesimal $\delta k = \frac{2\pi}{N_x a_x} \ll 2\pi$, we have:

$$\begin{aligned}
F_{i, i+1}^{mn} &= \langle m, k_{x,i}, k_y | n, k_{x, i+1}, k_y \rangle \\
&= \delta_{mn} + \langle m, k_{x,i}, k_y | (|n, k_{x, i+1}, k_y\rangle - |n, k_{x,i}, k_y\rangle) \\
&= \delta_{mn} - i A_{i, i+1}^{mn} \delta k \\
&\approx e^{-i A_{i, i+1}^{mn} \delta k} \quad (14)
\end{aligned}$$

where $A_{i,i+1}^{mn} = i \frac{\langle m, k_{x,i}, k_y | (|n, k_{x,i+1}, k_y\rangle - |n, k_{x,i}, k_y\rangle)}{\delta k}$ is the non-abelian $U(2N)$ gauge field. Hence we have that $D(k_y)$ is:

$$D(k_y) = \left[\prod_{i=0}^{N_x-1} F_{i,i+1} \right] = \left[\prod_{i=0}^{N_x-1} e^{-iA_{i,i+1}\delta k} \right] \\ = \left[P e^{\int_{C_{k_y}} -iA(k)dk} \right] \quad (15)$$

This is just the $U(2N)$ (not $SU(2N)$) Wilson loop, where the contour C_{k_y} is a contour at fixed k_y which goes across the BZ in k_x , i.e. goes from $k_x = -\pi$ to $k_x = \pi$, through $k_x = 0$.

The evolution of the Wannier function center for the effective 1D system with k_y can be easily obtained by looking at the phase factor θ_m^D . To see it more clearly, we fold θ axes and glue $\theta = -\pi$ line and $\theta = \pi$ line together. Then the Wannier function centers live on a cylinder surface, as shown in Fig.1. At $k_y = 0$, the eigenvalues of the D-matrix appear in degenerate pairs due to time reversal symmetry, which results in pairs of Wannier centers sitting at $k_y = 0$. When k_y moves away from the origin, the Wannier center pairs split and recombine at $k_y = \pi$ (where they again have to be degenerate due to time-reversal), as shown in Fig.1. Because θ_m^D is a phase factor, when two θ_m^D s meet together, they may differ by integer times of 2π . Therefore the evolution of each Wannier center pair will enclose the whole cylinder an integer times, which can be viewed as the winding number of the Wannier center pair. The Z_2 topological number is related to the summation of the winding numbers for all the pairs. If it is odd, then the Z_2 topological number is odd. It seems that the total winding number of the Wannier center pairs should generate an integer class Z instead of Z_2 . To clarify this point, let us look at the evolution of a Wannier center pair with winding number 4π . In that particular case, as shown in Fig.1(C), the pair of Wannier centers must have an extra "accidental" degeneracy between $k_y = 0$ and π , which is not protected by any symmetry and can be removed by "deforming" the Hamiltonian slightly to make the crossing of the levels become an anti-crossing as shown in Fig.1(C). The "deformation" process will thus change the total winding number by 4π and make it 0. Therefore only the total winding number mod 2 is a topological invariant.

Eq.(11) can be viewed as the discrete expression of the Wilson loop for the $U(2N)$ non-Abelian Berry's connection. It is obviously invariant under the $U(2N)$ gauge transformation and thus can be calculated directly from the wave functions obtained by first principle method without choosing any gauge fixing condition, which is the biggest advantage of the present form of the Z_2 invariance. From the discussion above one can see intuitively that the evolution of Wannier function obtained in this way agrees with the conclusion of Fu and Kane, although they are obtained in different approaches. We also find a rigorous proof of the equivalence of the topological invariant obtained in the current approach with the Z_2 number

proposed by Kane and Mele⁴, which is presented in the appendix.

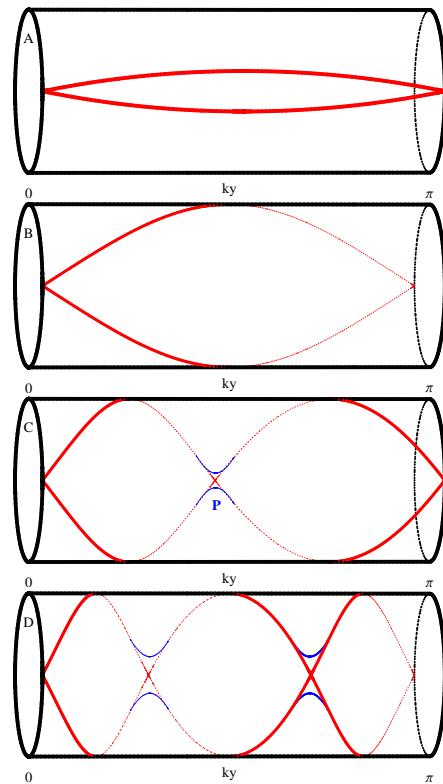


Figure 1: Schematic plots of the Wannier center curves: (A) for the trivial case, the Wannier center winding the cylinder zero times; (B) the Wannier center winding the cylinder one times; (C) the Wannier center winding the cylinder twice and the cross point labeled by P is not protected by time reversal symmetry and it is usually eliminated by some perturbation terms. (D) the Wannier center winding the cylinder 3 times, which is topologically equal to the case in B.

III. NUMERICAL RESULTS

In the present section, we will implement the method presented above and explicitly compute the Z_2 invariant for a series of systems. For each particular system, we calculate the evolution of the θ^D defined in equation(12) as the function of k_y from zero to π . The winding number of the Wannier center pairs defined in the above section can be checked in an equivalent way which is much simpler in practice. We first draw an arbitrary reference line parallel to the k_y axis, then compute the Z_2 number by counting how many times the evolution lines of the Wannier centers crosses the reference line.

A. BHZ model

Bernevig Hughes and Zhang (BHZ) showed that for an appropriate range of well thickness, the HgTe/CdTe

quantum well exhibits an inverted sub-band structure. In this inverted regime, the system exhibits a 2D QSHE¹³. BHZ introduce a simple four band tight binding model to describe this effect:

$$H_{eff}(k_x, k_y) = \begin{bmatrix} H(\mathbf{k}) & 0 \\ 0 & H^*(-\mathbf{k}) \end{bmatrix} \quad (16)$$

where $H(\mathbf{k}) = \varepsilon(\mathbf{k}) + d_i(\mathbf{k})\sigma_i$, $d_1 + id_2 = Aa^{-1}[\sin k_x a + i \sin k_y a]$, $d_3 = -2Ba^{-2}[2 - \frac{M}{2B} - \cos k_x a - \cos k_y a]$, $\varepsilon(\mathbf{k}) = C - 2Da^{-2}[2 - \cos k_x a - \cos k_y a]$. The constants A, B, C, D are given in the caption of Fig[2]. Below we take the lattice constant $a = 1$. The basis order is $|E_1+\rangle, |H_1+\rangle, |E_1-\rangle, |H_1-\rangle$ and the relevant subbands, $|E_1\pm\rangle$ and $|H_1\pm\rangle$ are two sets of Kramers' partners under the presence of time-reversal symmetry. H_{eff} consists of two decoupled blocks which are two copies of the massive Dirac Hamiltonian with a k -dependent mass $M(k)$. The coupling terms between blocks $|E_1+\rangle, |H_1+\rangle$ and $|E_1-\rangle, |H_1-\rangle$ will be induced by the breaking of inversion symmetry and were ignored in their original paper. When the effect of inversion symmetry breaking is taken into account, additional terms must be included in the effective model describing the mixing between the two blocks, which reads

$$H' = \begin{bmatrix} 0 & 0 & 0 & \Delta \\ 0 & 0 & -\Delta & 0 \\ 0 & -\Delta & 0 & 0 \\ \Delta & 0 & 0 & 0 \end{bmatrix} \quad (17)$$

The BHZ model has phase transition from normal insulator to topological insulator (QSH phase) when M changes sign from positive to negative. We then apply the new method to calculate the evolution pattern of the Wannier centers based on the above model Hamiltonian and show the results in Fig.2.

The corresponding results for the topological insulator phase in BHZ model are shown in Fig.2(A) with the parameters taken from reference¹³ as listed in the figure caption. When moving from $k_y = 0$ to π we see that the two evolution lines of Wannier centers enclose the cylinder once and equivalently these evolution lines cross the reference line (the red dashed line) only once. By contrast, for the normal insulator phase, as shown in Fig.2(B), the two evolution lines never cross the reference line. We emphasize that the reference line can be moved to somewhere else, but the even odd properties of the crossing numbers between the evolution lines and reference line will never change, which determines the Z_2 topological invariance. Therefore in the BHZ toy model for topological insulator, the Z_2 number calculated by our new method is consistent with the previous conclusion. Next we will apply the method to more realistic models of other topological insulator materials.

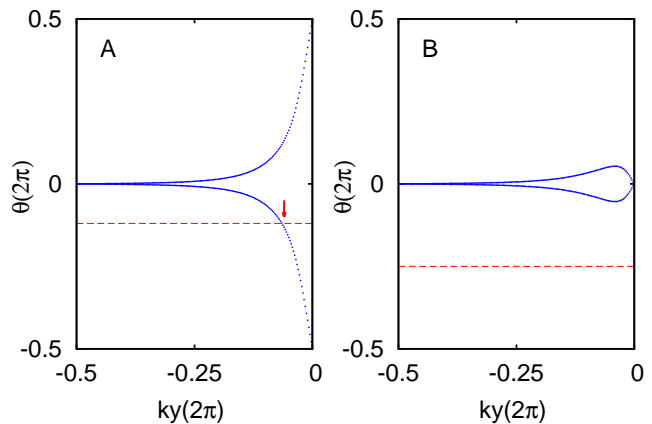


Figure 2: Wannier centers for the BHZ model. (A) For the QSH phase ($A=-13.68 \text{ eV} \cdot \text{\AA}$, $B=-16.9 \text{ eV} \cdot \text{\AA}^2$, $C=-0.0263 \text{ eV}$, $D=-0.514 \text{ eV} \cdot \text{\AA}^2$, $M=-2.058 \text{ eV}$, $\Delta=1.20 \text{ eV}$), The Wannier center cross the reference line (red dashed line) once (odd number of times); (B) For the Normal insulating phase ($A=-14.48 \text{ eV} \cdot \text{\AA}$, $B=-18.0 \text{ eV} \cdot \text{\AA}^2$, $C=-0.018 \text{ eV}$, $D=-0.594 \text{ eV} \cdot \text{\AA}^2$, $M=2.766 \text{ eV}$, $\Delta=1.20 \text{ eV}$), The Wannier center cross the reference line (red dashed line) zero (even number of) times.

B. CdTe and HgTe

The CdTe and HgTe materials have similar zinc-blende structure without bulk inversion symmetry. CdTe has a normal electronic structure, where the conduction bands (Γ_6) have the s-like character and the valance bands have the p-like character (Γ_8) through out the whole BZ. For HgTe, the band structure is inverted in a small area near the Γ point, where the s-like Γ_6 bands sink below the p-like Γ_8 bands. The band inversion at the Γ point changes the topological nature of the band structure and makes the HgTe to be a topological insulator if a true energy gap is opened by the lattice distortion⁴⁶(As pointed out in Ref.46, when the uniaxial strain is applied along the [001] direction for HgTe by choosing the ratio of lattice constants c/a to be 0.98, an energy gap about 0.05eV is opened at the Γ point). We then use the tight-binding model⁴⁷ to calculate the pattern of the Wannier center evolution θ defined in Eq.12 and show the results in Fig.3. We investigate the topological properties of 3D bulk system by checking two planes in the k space, namely the planes with $k_z = 0$ and $k_z = \pi$. It is clear that in the HgTe system, for $k_z = 0$ the evolution lines cross the reference line (red dashed line) once (as shown in Fig.3(A)), while for $k_z = \pi$ they never cross it (as shown in Fig.3(B)). The above results indicate that for HgTe the effective 2D systems with $k_z = 0$ and π are effectively 2D topological insulator and normal insulator respectively, which determines HgTe to be a strong 3D topological insulator¹⁵. A similar analysis can be also applied to CdTe and the results are shown in Fig.3(C) and (D), indicating CdTe to be a normal insulator.

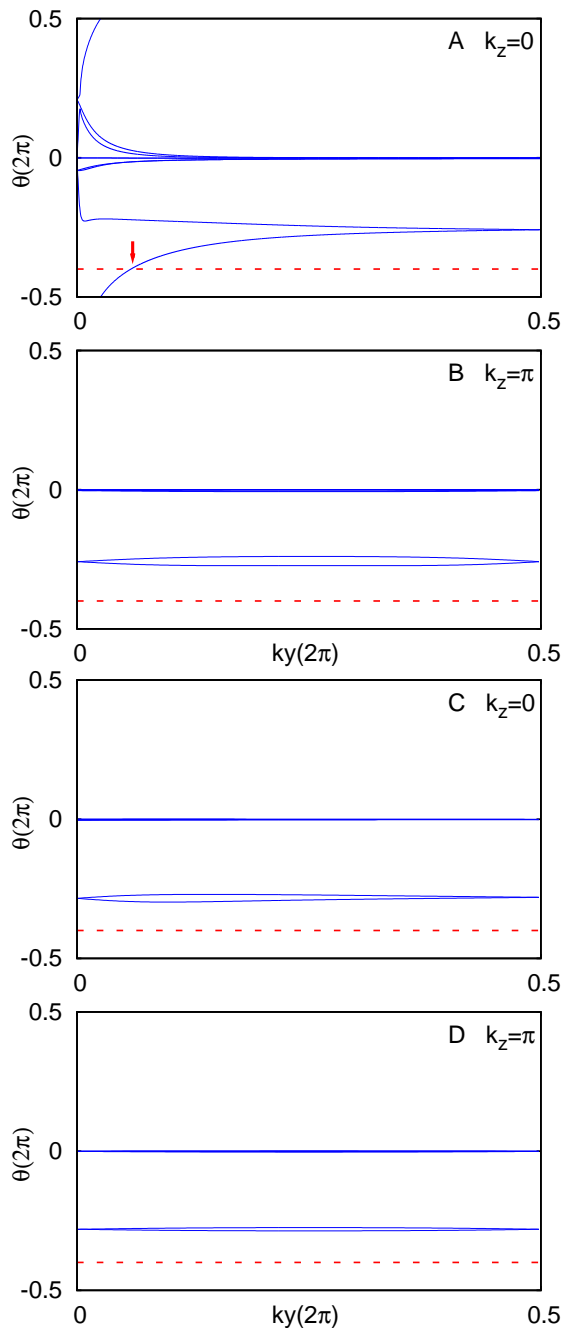


Figure 3: The evolution lines of Wannier centers for HgTe (A, B) and CdTe (C, D). For HgTe system, The evolution lines cross the reference line odd number of times in the $k_z = 0$ plane and even times in the $k_z = \pi$ plane, indicating HgTe is a strong topological insulator. For CdTe, the evolution lines cross the reference line zero times for both $k_z = 0$ and π planes, indicating CdTe is a normal insulator.

C. Bi_2Se_3 system

Recently, the tetradymite semiconductors Bi_2Te_3 , Bi_2Se_3 , and Sb_2Te_3 have been theoretically predicted and experimentally observed to be topological insulators with a bulk band gap as large as 0.3eV in Bi_2Se_3 ^{20,21,23,25,26,39}.

The surface states in Bi_2Se_3 have been found by both ARPES^{21,23} and STM³⁶, which are consistent with the theoretical results²⁰.

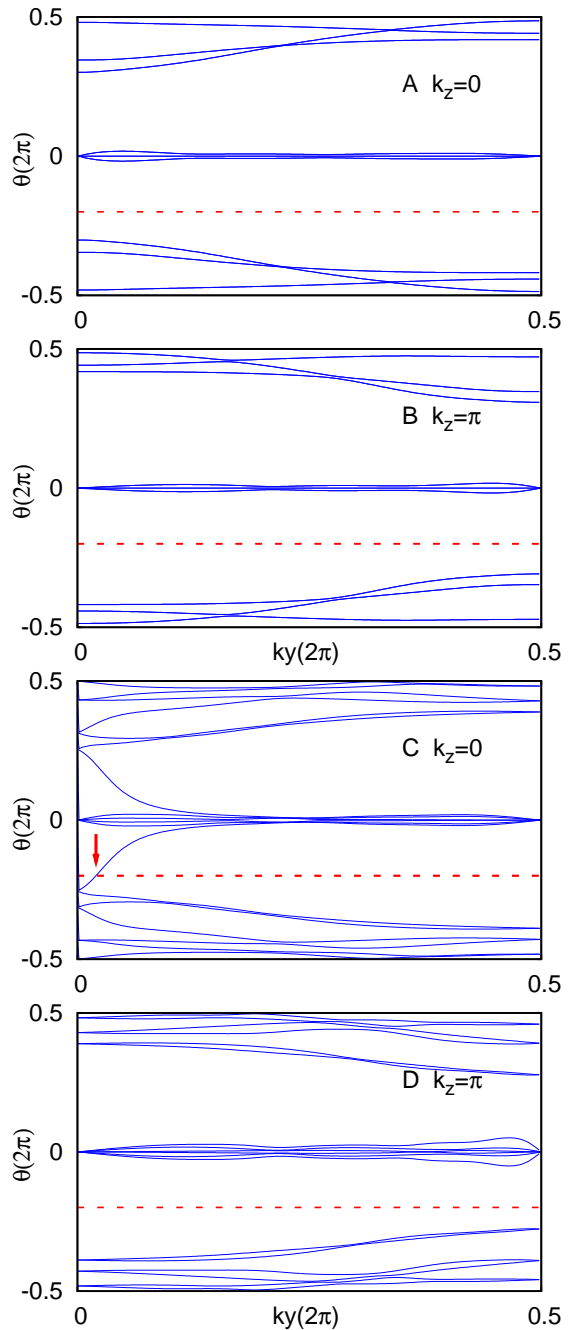


Figure 4: The evolution lines of Wannier centers for Bi_2Se_3 system without (A, B) and with SOC (C, D). If we turn off SOC the system is a normal insulator and the evolution lines never cross the reference line for both $k_z = 0$ and π planes as shown in (A) and (B), indicating the system to be a normal insulator. When the SOC is turned on the system is in a strong topological insulator phase, and the evolution lines cross the reference line odd number of times in $k_z = 0$ and even number of times in $k_z = \pi$ plane as shown in (C) and (D), indicating the system is topologically non-trivial.

Since the Bi_2Se_3 family has inversion symmetry, the Z_2 topological number can be easily calculated by the production of the parities at each high symmetry points in the BZ¹⁶. Below we apply our new method to calculate the topological properties of this system, using the tight binding model obtained in reference²⁰. We first perform the calculation for the Bi_2Se_3 without spin-orbit coupling (SOC): the results are shown in Fig.4(A,B). It is clear that the evolution lines never cross the reference line for both $k_z = 0$ and π , indicating that the system is topologically trivial without SOC. When the realistic SOC is turned on, as shown in Fig.4(C,D), the evolution lines cross the reference line once only in the case of $k_z = 0$ but not for $k_z = \pi$ indicating the Bi_2Se_3 bulk material is a 3D strong topological insulator.

D. Bi_2Te_3 slab system

As calculated by Liu et al⁴⁸, upon reducing the thickness of Bi_2Te_3 and Bi_2Se_3 films, the topological nature of the system alternates between topologically trivial and non-trivial behavior as a function of the layer thickness. Liu et al. pointed out that the 1QL Bi_2Te_3 slab is a trivial insulator and 2QL Bi_2Te_3 slab is a 2D topological insulator⁴⁸. We apply our method to these systems. The evolution patterns for the 1QL and 2QL Bi_2Te_3 slabs are obtained using the tight binding Hamiltonian developed in references^{48,49} and the results are summarized in Fig.5. In the 1QL slab system (Fig.5(A)), the evolution pattern appears in a trivial manner while that of the 2QL slab system is non-trivial(Fig.5(B)). This is consistent with the conclusion based on the parity counting⁴⁸.

E. Bi and Sb system

Murakami pointed out that the Z_2 topological number is odd in the 2D bilayer bismuth system⁵⁰. We apply our method to this system using the tight-binding model developed in Ref.51, which faithfully reproduces the bulk bismuth band structure. As shown in Fig.6A, the band structure of bilayer bismuth is topologically nontrivial, which is quite consistent with the previous conclusion⁵⁰. After that we apply the same method to calculate bilayer Sb, which has the similar lattice structure as bismuth, but with relatively weak SOC. As plotted in Fig.6(B), the evolution pattern of bilayer Sb shows clearly that it is in the normal insulator phase, which is also consistent with the parity counting.

F. Graphene system

Graphene consists of a honeycomb lattice of carbon atoms with two sites per unit cell. Kane and Mele introduced a tight-binding model which generalizes Haldane's

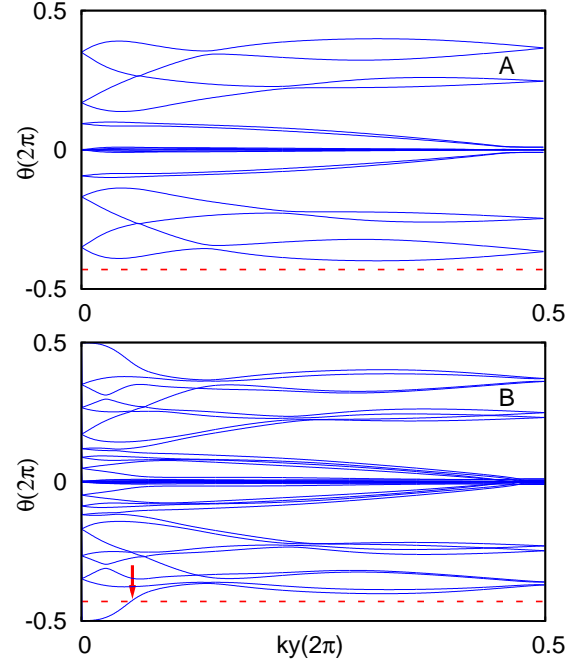


Figure 5: The evolution lines of Wannier centers for 1QL and 2QL Bi_2Te_3 slab. (A) The 1QL Bi_2Te_3 slab is in normal insulator phase. (B) The 2QL Bi_2Te_3 slab is in topological insulator phase.

model to include spin with time reversal invariant spin-orbit interactions⁴:

$$\begin{aligned}
 H = t \sum_{\langle i,j \rangle, \sigma} c_{i,\sigma}^\dagger c_{j,\sigma} + i\lambda_{so} \sum_{\langle\langle i,j \rangle\rangle, \sigma\sigma'} \nu_{ij} c_{i,\sigma}^\dagger s_{\sigma\sigma'}^z c_{j,\sigma'} \\
 + i\lambda_R \sum_{\langle i,j \rangle, \sigma\sigma'} c_{i,\sigma}^\dagger (\mathbf{s}_{\sigma\sigma'} \times \hat{\mathbf{d}}_{ij})_z c_{j,\sigma'} + \lambda_v \sum_{i,\sigma} \xi_i c_{i,\sigma}^\dagger c_{i,\sigma}
 \end{aligned} \tag{18}$$

where i, j are the site indices and σ, σ' are the spin indices and t is the nearest-neighbor hopping amplitude. In the second term, λ_{so} is the strength of SOC between second neighbors, with $\nu_{ij} = (2/\sqrt{3})[\hat{\mathbf{d}}_1 \times \hat{\mathbf{d}}_2]_z = \pm 1$ depending on the relative orientation of the first-neighbor bond vectors $\hat{\mathbf{d}}_1$ and $\hat{\mathbf{d}}_2$ encountered by an electron hopping from site j to site i , and s_z is the z Pauli spin matrix. The third term is a nearest neighbor Rashba term, which breaks the $z \rightarrow -z$ mirror symmetry, and can be generated by a perpendicular electric field or interaction with the substrate. The fourth term is a staggered sublattice potential, where ξ_i equals $+1$ and -1 on A and B sites respectively. In what follows we use t as the energy scale and fix $\lambda_{so} = 0.06t$ and $\lambda_R = 0.05t$. Varying the parameter λ_v allows us to switch from normal insulator to QSH phase. In the present study, we choose $\lambda_v = 0.1t$ for the QSH phase and $\lambda_v = 0.4t$ for the normal insulating phase. The calculated Wannier centers evolution patterns are shown in Fig.7. It can be easily found that the evolution lines cut the reference line only once in Fig.7(A) but not in Fig.7(B) indicating the former is topologically

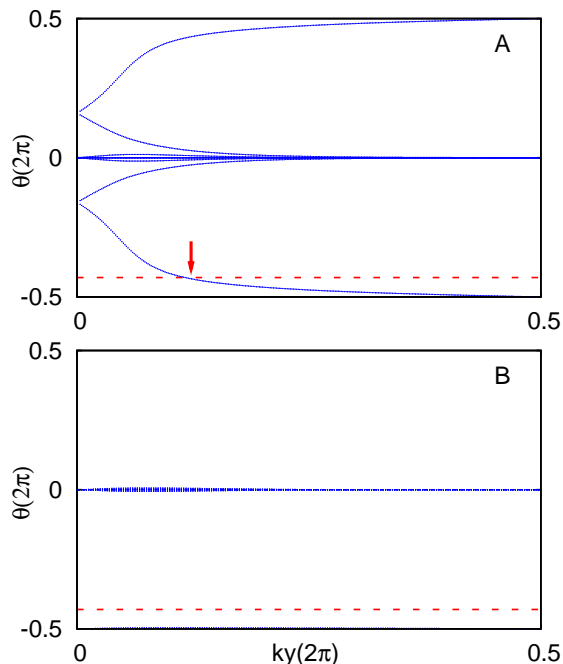


Figure 6: The evolution lines of Wannier centers for 2D bilayer Bi (A) and Sb (B) system, indicating the bilayer Bi is topologically nontrivial but Sb is topologically trivial.

non trivial and the latter is trivial.

In conclusion, we have proposed a new equivalent expression for the Z_2 topological invariance using the $U(2N)$ non-Abelian Berry connection. Based on this new expression we calculated the evolution of the Wannier function center for several topological and normal insulating systems with or without inversion symmetry. We showed that for the nontrivial topological insulators, the Wannier function center have partner switching patterns, topologically different from the normal (trivial) insulating systems. Additionally, we gave a proof that the new method is equivalent to the Z_2 number proposed by Fu and Kane.

Note During the preparation of this manuscript, we noticed the paper by Soluyanov and Vanderbilt⁵², where the construction of Wannier functions for Z_2 topological insulators are discussed from a different point of view. We addressed in this paper that the real construction of Wannier functions is not necessary, while only the "Wannier representation" and corresponding Berry connection evaluated along the "Wilson loop" are essential keys in order to identify the topological nature. And at the same time there is another paper by Zohar Ringel and Yaacov E. Kraus⁵³, which determine the Z_2 invariant in a way that does not require any gauge fixing and lead to similar conclusions as ours.

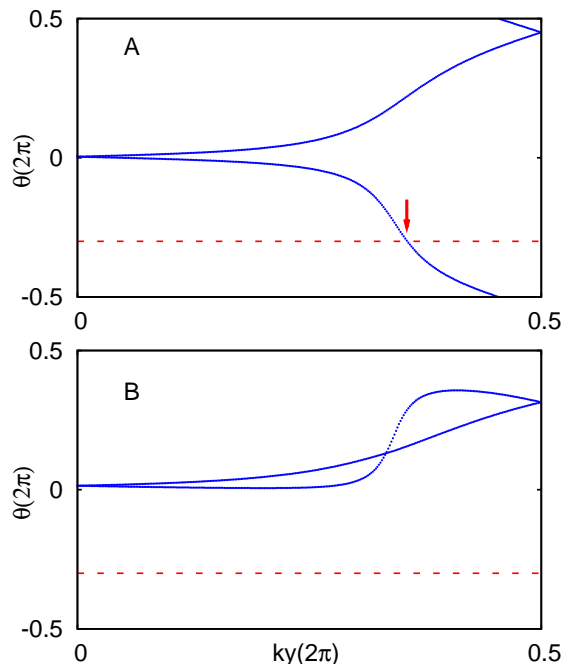


Figure 7: The evolution lines of Wannier center for graphene in the (A) QSH phase $\lambda_v = 0.1t$ and (B) the normal insulating phase $\lambda_v = 0.4t$. In both cases $\lambda_{SO} = 0.06t$ and $\lambda_R = 0.05t$.

Acknowledgments

BAB was supported by Princeton Startup Funds, Alfred P. Sloan Foundation, NSF DMR-095242, and NSF China 11050110420, and MRSEC grant at Princeton University, NSF DMR-0819860. XLQ is partly supported by Alfred P. Sloan Foundation. BAB and XLQ thank the Institute of Physics in Beijing, China for generous hosting. XD and ZF acknowledge the supports from NSF of China and that from the 973 program of China (No.2007CB925000)

Appendix A: Wilson loop and pfaffian topological invariant

In this section, we will prove that the $U(2)$ Wilson loop is related to the Pfaffian topological invariant of time-reversal topological insulators. In a system with time-reversal invariant we can relate the bands at k and $-k$ through a unitary matrix B ,

$$|n, -k\rangle = B_{nm}^*(k) \hat{T} |m, k\rangle \quad (\text{A1})$$

with $B(k)$ unitary and has the property:

$$B(-k) = -B^T(k) \quad (\text{A2})$$

We have the following relation between F_{k_1, k_2} matrices:

$$\begin{aligned}
F_{-k_2, -k_1}^{mn} &= \langle m, -k_2 | n, -k_1 \rangle \\
&= \langle m', k_2 | \hat{T} B_{mm'}(k_2) B_{nn'}^*(k_1) \hat{T} | n', k_1 \rangle \\
&= B_{mm'}(k_2) B_{nn'}^*(k_2) F_{k_1, k_2}^{n'm'}
\end{aligned} \tag{A3}$$

or equivalently:

$$F_{-k_2, -k_1} = B(k_2) F_{k_1, k_2}^T B^\dagger(k_1) \tag{A4}$$

We now focus on the $k_y = 0$ or $k_y = \pi$ paths (say $k_y = 0$), each of which has k_x going from $-\pi$ to π , so that $k_y = -k_y$, and compute the finite difference:

$$\begin{aligned}
D(k_y = 0) &= \prod_{i=0}^{N_x-1} F_{i, i+1} \\
&= F_{-\frac{N_x}{2}\Delta k, -(\frac{N_x}{2}-1)\Delta k} \cdots F_{(\frac{N_x}{2}-1)\Delta k, \frac{N_x}{2}\Delta k}
\end{aligned} \tag{A5}$$

All the F 's in the above equation are considered at $k_y = 0$, and the k in the above expresses the k_x coordinate. By eq.(A4), we have:

$$F_{-\Delta k, 0} = B(\Delta k) F_{0, \Delta k}^T B^\dagger(0),$$

$$F_{-2\Delta k, -\Delta k} = B(2\Delta k) F_{\Delta k, 2\Delta k}^T B^\dagger(\Delta k), \cdots \tag{A6}$$

Hence the Wilson loop above becomes:

$$\begin{aligned}
D &= B\left(\frac{N_x}{2}\Delta k\right) F_{(\frac{N_x}{2}-1)\Delta k, \frac{N_x}{2}\Delta k}^T B^\dagger\left(\left(\frac{N_x}{2}-1\right)\Delta k\right) \cdots \\
&\times B(2\Delta k) F_{\Delta k, 2\Delta k}^T B^\dagger(\Delta k) B(\Delta k) F_{0, \Delta k}^T B^\dagger(0) F_{0, \Delta k} \\
&\times F_{\Delta k, 2\Delta k} F_{2\Delta k, 3\Delta k} \cdots F_{(\frac{N_x}{2}-1)\Delta k, \frac{N_x}{2}\Delta k} \\
&= B\left(\frac{N_x}{2}\Delta k\right) F_{(\frac{N_x}{2}-1)\Delta k, \frac{N_x}{2}\Delta k}^T F_{(\frac{N_x}{2}-2)\Delta k, (\frac{N_x}{2}-1)\Delta k}^T \cdots \\
&\times F_{\Delta k, 2\Delta k}^T F_{0, \Delta k}^T B^\dagger(0) F_{0, \Delta k} F_{\Delta k, 2\Delta k} F_{2\Delta k, 3\Delta k} \cdots \\
&\times F_{(\frac{N_x}{2}-2)\Delta k, (\frac{N_x}{2}-1)\Delta k} F_{(\frac{N_x}{2}-1)\Delta k, \frac{N_x}{2}\Delta k}
\end{aligned} \tag{A7}$$

where we have used the fact that $B^\dagger(k)B(k) = I$ (unitary matrix). We see that all the intermediate B matrices vanish with the exception of the ones at the inversion symmetric points $0, \frac{N_x}{2}\Delta k = \pi$. This is true for any time-reversal invariant contour. Moreover, it is suggestive that the two left-over matrices $B^\dagger(0), B(\frac{N_x}{2}\Delta k)$ should be brought together, so we must commute $B^\dagger(0)$ all across the matrix chain. The matrix $B(0)$ (and $B(\pi)$) has the property that it is unitary and antisymmetric (eq(A2)). We then know it has to be of the form:

$$B(0) = e^{i\theta} \sigma_2 \tag{A8}$$

The matrix F_{k_1, k_2} , for $k_2 - k_1 \ll \pi$, as show in eq(14), has the following form:

$$F_{k_1, k_2}^{mn} = \delta_{mn} - i A_{k_1, k_2}^{mn}(k_2 - k_1) \tag{A9}$$

where $k_2 - k_1 = \Delta k$. We decompose the $U(2)$ gauge field into its abelian and non-abelian part:

$$A_{k_1, k_2}^{mn} = A_{k_1, k_2}^{U(1)} \delta_{mn} + A_{k_1, k_2}^{SU(2), i} (\sigma^i)_{mn} \tag{A10}$$

where $i = 1, 2, 3$ and double index implies summation. $A_{k_1, k_2}^{U(1)}, A_{k_1, k_2}^{SU(2), i}$ are numbers. We then have:

$$\begin{aligned}
(F_{k_1, k_2}^T) B^\dagger(0) &= B^\dagger(0) (I - i A_{k_1, k_2}^{U(1)} (k_2 - k_1) I) \\
&\quad - i A_{k_1, k_2}^{SU(2), i} (\sigma^i)^T (k_2 - k_1) B^\dagger(0)
\end{aligned} \tag{A11}$$

We aim to commute the matrix B with the Pauli matrices of the nonabelian vector potential. We use the identities $\sigma_x^T \sigma_y = -\sigma_y \sigma_x$, $\sigma_y^T \sigma_y = -\sigma_y \sigma_y$, $\sigma_z^T \sigma_y = -\sigma_y \sigma_z$ and hence:

$$\begin{aligned}
A_{k_1, k_2}^{SU(2), i} (\sigma^i)^T B^\dagger(0) &= e^{-i\theta} A_{k_1, k_2}^{SU(2), i} (\sigma^i)^T \sigma_2 \\
&= -e^{-i\theta} \sigma_2 A_{k_1, k_2}^{SU(2), i} \sigma^i = -B^\dagger(0) A_{k_1, k_2}^{SU(2), i} \sigma^i
\end{aligned} \tag{A12}$$

Hence:

$$\begin{aligned}
(F_{k_1, k_2}^T) B^\dagger(0) &= B^\dagger(0) [I + i (A_{k_1, k_2}^{U(1)} I + A_{k_1, k_2}^{SU(2), i} \sigma^i) (k_2 - k_1) \\
&\quad - i 2 A_{k_1, k_2}^{U(1)} I (k_2 - k_1)]
\end{aligned} \tag{A13}$$

We also have

$$\begin{aligned}
I + i (A_{k_1, k_2}^{U(1)} I + A_{k_1, k_2}^{SU(2), i} \sigma^i) (k_2 - k_1) &- 2i A_{k_1, k_2}^{U(1)} I (k_2 - k_1) \\
&= I + i (A_{k_1, k_2})^\dagger (k_2 - k_1) - 2i A_{k_1, k_2}^{U(1)} (k_2 - k_1) I \\
&\approx F_{k_1, k_2}^\dagger e^{-2i A_{k_1, k_2}^{U(1)} (k_2 - k_1)}
\end{aligned} \tag{A14}$$

where in the limit of $k_2 - k_1 \ll 2\pi$ (the case in all our terms) we neglect $(k_2 - k_1)^2$ order terms, and where A_{k_1, k_2} is the full $U(2)$ field strength. We have also used the fact that A is an anti-hermitian matrix $A_{k_1, k_2}^{mn}(k_2 - k_1) = -(A_{k_1, k_2}^{nm})^*(k_2 - k_1)$. After all this long detour, we have proved:

$$F_{k_1, k_2}^T B^\dagger(0) = B^\dagger(0) F_{k_1, k_2}^\dagger e^{-2i A_{k_1, k_2}^{U(1)} (k_2 - k_1)} \tag{A15}$$

We then return to the $U(2)$ Wilson loop.

$$\begin{aligned}
D &= B\left(\frac{N_x}{2}\Delta k\right) F_{\left(\frac{N_x}{2}-1\right)\Delta k, \frac{N_x}{2}\Delta k}^T F_{\left(\frac{N_x}{2}-2\right)\Delta k, \left(\frac{N_x}{2}-1\right)\Delta k}^T \\
&\times F_{\left(\frac{N_x}{2}-3\right)\Delta k, \left(\frac{N_x}{2}-2\right)\Delta k}^T F_{\left(\frac{N_x}{2}-4\right)\Delta k, \left(\frac{N_x}{2}-3\right)\Delta k}^T \cdots \\
&\times F_{\Delta k, 2\Delta k}^T F_{0, \Delta k}^T B^\dagger(0) F_{0, \Delta k} F_{\Delta k, 2\Delta k} F_{2\Delta k, 3\Delta k} \cdots \\
&\times F_{\left(\frac{N_x}{2}-2\right)\Delta k, \left(\frac{N_x}{2}-1\right)\Delta k} F_{\left(\frac{N_x}{2}-1\right)\Delta k, \frac{N_x}{2}\Delta k} \\
&= e^{-2i(A_{0, \Delta k}^{U(1)} + A_{\Delta k, 2\Delta k}^{U(1)} + A_{2\Delta k, 3\Delta k}^{U(1)} + \cdots + A_{(N_x/2-1)\Delta k, (N_x/2)\Delta k}^{U(1)})\Delta k} \\
&\times B\left(\frac{N_x}{2}\Delta k\right) B^\dagger(0) \quad (A16)
\end{aligned}$$

where we have used $U_{0, \Delta k}^\dagger U_{0, \Delta k} = U_{\Delta k, 2\Delta k}^\dagger U_{\Delta k, 2\Delta k} = I$, etc.... Hence:

$$D = e^{-2i(A_{0, \Delta k}^{U(1)} + A_{\Delta k, 2\Delta k}^{U(1)} + \cdots + A_{(N_x/2-1)\Delta k, (N_x/2)\Delta k}^{U(1)})\Delta k} B(\pi) B^\dagger(0)$$

We note that the phase above is twice the $U(1)$ (matrix, not traced) phase picked up from 0 to π . Lets re-define it by re-expressing it from $-\pi$ to π . i.e. the full abelian Berry for the interval considered. We have

$$\begin{aligned}
A_{-k_2, -k_1}^{U(1)} \Delta k &= \frac{i}{2} \text{tr}[F_{-k_2, -k_1} - I] \\
&= \frac{i}{2} \text{tr}[B(k_2) F_{k_1, k_2}^T B^\dagger(k_1) - I] \quad (A17)
\end{aligned}$$

where we have used eq(A4). Since $k_2 - k_1 \ll 2\pi$, we can approximate $B(k_2) - B(k_1)$ as small and write $B(k_2) = B(k_1) + B(k_2) - B(k_1)$ to get:

$$\begin{aligned}
A_{-k_2, -k_1}^{U(1)} \Delta k &= \frac{i}{2} \text{tr}[B(k_1) F_{k_1, k_2}^T B^\dagger(k_1) - I] \\
&+ (B(k_2) - B(k_1)) F_{k_1, k_2}^T B^\dagger(k_1) \\
&= \frac{i}{2} \text{tr}[F_{k_1, k_2}^T - I + (B(k_2) - B(k_1)) F_{k_1, k_2}^T B^\dagger(k_1)] \\
&= A_{k_1, k_2}^{U(1)} \Delta k + \frac{i}{2} \text{tr}[(B(k_2) - B(k_1)) F_{k_1, k_2}^T B^\dagger(k_1)] \quad (A18)
\end{aligned}$$

As $B(k_2) - B(k_1)$ is considered small for $k_2 - k_1 \ll 2\pi$, we take

$$(B(k_2) - B(k_1)) F_{k_1, k_2}^T \approx B(k_2) - B(k_1) \quad (A19)$$

where we took $F_{k_1, k_2}^T \approx I$ if multiplied by another small number. Hence:

$$A_{-k_2, -k_1}^{U(1)} \Delta k = A_{k_1, k_2}^{U(1)} \Delta k + \frac{i}{2} \text{tr}[(B(k_2) - B(k_1)) B^\dagger(k_1)] \quad (A20)$$

We then find:

$$\begin{aligned}
&2(A_{0, \Delta k}^{U(1)} + A_{\Delta k, 2\Delta k}^{U(1)} + \cdots + A_{(N_x/2-1)\Delta k, (N_x/2)\Delta k}^{U(1)})\Delta k \\
&= (A_{-(N_x/2)\Delta k, -(N_x/2-1)\Delta k}^{U(1)} + \cdots + A_{-\Delta k, 0}^{U(1)} \\
&+ A_{0, \Delta k}^{U(1)} + \cdots + A_{(N_x/2-1)\Delta k, (N_x/2)\Delta k}^{U(1)})\Delta k \\
&- \frac{i}{2} \int_0^\pi dk \text{tr}[B^\dagger(k) \nabla_k B(k)] \quad (A21)
\end{aligned}$$

The first term is just the $U(1)$ phase in the contour direction: $\int_{-\pi}^\pi A^{U(1)}(k) dk$. The Wilson loop is then:

$$W = e^{\int_{-\pi}^\pi -iA^{U(1)}(k) dk - \frac{i}{2} \int_0^\pi dk \text{tr}[B^\dagger(k) \nabla_k B(k)]} \cdot B(\pi) B^\dagger(0) \quad (A22)$$

As $B(k)$ is unitary, we also know that $\text{tr}[B^\dagger(k) \nabla_k B(k)] = \nabla_k \log \det B(k)$ and hence:

$$e^{-\frac{i}{2} \int_0^\pi dk \text{tr}[B^\dagger(k) \nabla_k B(k)]} = e^{-\frac{i}{2} \log \left[\frac{\det B(\pi)}{\det B(0)} \right]} = \sqrt{\frac{\det B(0)}{\det B(\pi)}} \quad (A23)$$

The Wilson loop becomes:

$$D = e^{\int_{-\pi}^\pi -iA^{U(1)}(k) dk} \cdot \sqrt{\frac{\det B(0)}{\det B(\pi)}} \cdot B(\pi) B^\dagger(0) \quad (A24)$$

As we said before, $B(0)$, $B(\pi)$ are unitary, 2 by 2 matrices, antisymmetric, so:

$$B(0) = Pf(B(0)) \begin{bmatrix} 0 & 1 \\ -1 & 0 \end{bmatrix} \quad (A25)$$

and similarly for $B(\pi)$

where Pf is the pfaffian of the matrix. We hence have:

$$D = e^{\int_{-\pi}^\pi -iA^{U(1)}(k) dk} \sqrt{\frac{\det B(0)}{\det B(\pi)} \frac{Pf(B(\pi))}{Pf(B(0))}} I \quad (A26)$$

where I is the 2×2 identity matrix.

We now make several observations. Obviously, the above equality is valid on both time-reversal invariant lines at $k_y = 0$ and $k_y = \pi$, i.e. we can define two Wilson loops:

$$\begin{aligned}
D(k_y = 0) &= e^{\int_{-\pi}^\pi -iA^{U(1)}(k_x, k_y=0) dk_x} \\
&\times \sqrt{\frac{\det B(0,0)}{\det B(\pi,0)} \frac{Pf(B(\pi,0))}{Pf(B(0,0))}} I \quad (A27)
\end{aligned}$$

and similarly for momentum π .

Second, we notice that the $U(1)$ phase factor is not just the usual abelian Berry phase but only *half* of it. Indeed, as per our definition:

$$A_{k_1, k_2}^{m, n} = A_{k_1, k_2}^{U(1), i} \delta_{mn} + A_{k_1, k_2}^{SU(2), i} (\sigma^i)_{mn} \quad (A28)$$

This implies:

$$A_{\vec{k}}^{U(1),i} = \frac{1}{2} \sum_m \langle m, \vec{k} | m, \vec{k} \rangle \quad (\text{A29})$$

which has a $1/2$ difference from the usual form. This difference is actually important. Define:

$$\Phi(k_y) = \oint_{-\pi}^{\pi} dk_x A_x(k_x, k_y) = i \log \det D(k_y) \quad (\text{A30})$$

We then have:

$$\begin{aligned} \int_0^{\pi} \nabla_{k_y} \Phi(k_y) &= \int_0^{\pi} i \nabla_{k_y} \log \det D(k_y) \\ &= \Phi(\pi) - \Phi(0) + 2\pi M_n \end{aligned} \quad (\text{A31})$$

where M_n is the winding number of the phase $\Phi(k_y)$. The phase $\Phi(k_y)$ is the sum of the phases $\phi_1(k_y)$ and $\phi_2(k_y)$ of the two eigenvalues of the Wilson loop *both defined in the interval* $[0, 2\pi]$. Each of these eigenvalues has a winding number which adds to M_n , and the system will turn to be nontrivial if the system has a odd M_n . We now take the Wilson loop W from $k_x = -\pi, \pi$ at $k_y = 0$, and then from $k_x = \pi, -\pi$ at $k_y = \pi$:

$$\begin{aligned} W &= D(k_y = 0)(D(k_y = \pi))^{-1} \\ &= e^{\frac{i}{2}(\Phi(0) - \Phi(\pi))} \times \prod_{i=\vec{G}_i/2} \frac{\sqrt{\text{Det}B(\vec{G}_i/2)}}{\text{Pf}(B(\vec{G}_i/2))} \\ &= e^{\frac{i}{2}(-\int_0^{\pi} \nabla_{k_y} \log \det D(k_y)) - \pi i M_n} \prod_{i=\vec{G}_i/2} \frac{\sqrt{\text{Det}B(\vec{G}_i/2)}}{\text{Pf}(B(\vec{G}_i/2))} \end{aligned}$$

$\vec{G}_i/2$ are the time-reversal invariant momenta $(0, 0), (0, \pi), (\pi, 0), (\pi, \pi)$. As such:

$$\begin{aligned} D(k_y = 0) &= e^{\frac{i}{2}(\int_0^{\pi} \nabla_{k_y} \log \det D(k_y))} (D(k_y = \pi))^{-1} \\ &= e^{-\pi i M_n} \prod_{i=\vec{G}_i/2} \frac{\sqrt{\text{Det}B(\vec{G}_i/2)}}{\text{Pf}(B(\vec{G}_i/2))} \end{aligned} \quad (\text{A32})$$

We have proved that both $D(k_y = 0)$ and $D(k_y = \pi)$ are proportional to unity matrix, up to a sign. For a smooth gauge, the difference in sign is taken by the contour term $e^{\frac{i}{2}(\int_0^{\pi} \nabla_{k_y} \log \det D(k_y))}$ to give

$$D(k_y = 0) e^{\frac{i}{2}(\int_0^{\pi} \nabla_{k_y} \log \det D(k_y))} (D(k_y = \pi))^{-1} = I \quad (\text{A33})$$

to give

$$e^{\pi i M_n} = \prod_{i=\vec{G}_i/2} \frac{\sqrt{\text{Det}B(\vec{G}_i/2)}}{\text{Pf}(B(\vec{G}_i/2))} \quad (\text{A34})$$

which says that the pfaffian invariant is just the parity of the band switch number M_n . For M_n odd, it is nontrivial. Note that although our proof above is explicit only

for two occupied bands, it can be easily extended to the $2N_{\text{occupied}}$ band case when we realize that that case is just a tensor product (upon removing accidental degeneracies) of N_{occupied} time-reversal invariant multiplets for which the above expression applies.

Appendix B: Wilson loop and the Z_2 invariant expressed as an obstruction

An alternative formulation of the Z_2 invariant has been defined by Fu and Kane⁷, where the Z_2 invariant is expressed as an obstruction of the $U(1)$ Berry's phase gauge field in half of the BZ. This approach has some convenience in its similarity with the Chern number formula of the quantum Hall states by Thouless *et al*². The application of this approach to numerical calculation of the Z_2 invariant in finite size systems has been studied by Fukui and Hatsugai¹⁸. Here we provide an alternative proof of the relation between our Wilson loop approach and the Z_2 invariant through the obstruction formula. We start by reviewing the obstruction formulation of Fu and Kane⁷ (Appendix A1). Consider $|n, k\rangle$ as the occupied Bloch bands. We make the gauge choice

$$|n, -k\rangle = \mathcal{T}_{nm} T(|m, k\rangle) \quad (\text{B1})$$

with \mathcal{T} an antisymmetric matrix satisfying $\mathcal{T}^2 = -1$. Comparing to Eq. (A1), the gauge choice here corresponds to the requirement that $B_{nm}(k)$ is independent from k . More explicitly, with $2N$ occupied bands we can label the bands in pairs as $|n, k\rangle$ and $|\bar{n}, k\rangle$ with $n = 1, \dots, N$. Time-reversal acts as $|\bar{n}, -k\rangle = T|n, k\rangle$, $|n, -k\rangle = -T|\bar{n}, k\rangle$. so that the wavefunctions in the lower half BZ defined by $k_y \in [-\pi, 0]$ is determined by those in the upper half BZ, denoted by $\tau_{1/2}$. With this gauge choice, for topological insulator it is not possible to make a continuous and single-valued choice of the wavefunctions in the whole BZ. However, it is always possible to define the wavefunctions continuously in the half BZ $\tau_{1/2}$, so that all obstructions are pushed to the boundary between the two half BZs, *i.e.* the two lines $k_y = 0$ and $k_y = \pi$. In such a gauge choice, Fu and Kane shows that the Z_2 invariant is given by an obstruction in the half BZ:

$$\Delta = \frac{1}{2\pi} \left(\oint_{\partial\tau_{1/2}} \mathbf{a} \cdot d\mathbf{l} - \int_{\tau_{1/2}} d^2k F_{xy} \right) \text{ mod } 2 \quad (\text{B2})$$

where $a_i = i \sum_n \langle nk | \partial_i | nk \rangle$ is the $U(1)$ part of the Berry phase connection. By first integrating over k_x and define the $U(1)$ Wilson loop

$$\Phi(k_y) = \oint_{-\pi}^{\pi} dk_x a_x(k_x, k_y) \quad (\text{B3})$$

The Z_2 invariant can be expressed as

$$\Delta = \frac{1}{2\pi} \left(\int_0^\pi dk_y \partial_{k_y} \Phi(k_y) - (\Phi(\pi) - \Phi(0)) \right) \text{ mod } 2 \quad (\text{B4})$$

If we do not have any restriction on the gauge choice (other than requiring that the wavefunctions be continuous in $\tau_{1/2}$ so that $\Phi(k_y)$ is continuous and well-defined), Δ can be 0, or any arbitrary integer. However, the gauge choice eq.(B1) removes this ambiguity. Consider the states $|nk\rangle$ for $k_y = 0$. A gauge transformation

$$|nk\rangle \rightarrow e^{i\varphi_{\mathbf{k}}} |nk\rangle \quad (\text{B5})$$

corresponds to a gauge transformation $\mathbf{A} \rightarrow \mathbf{A} + \nabla_{\mathbf{k}}\varphi$, where $A_i^{nm} = i\langle nk|\partial_i|mk\rangle$, which leads to the change in the flux

$$\Phi(k_y = 0) \rightarrow \Phi(k_y = 0) + 2N \oint_{-\pi}^{\pi} dk_x \partial_x \varphi_{k_x,0} \quad (\text{B6})$$

However, to preserve the condition eq.(B1) we have to require

$$\varphi_{\mathbf{k}} = -\varphi_{-\mathbf{k}} \quad (\text{B7})$$

so that

$$\oint_{-\pi}^{\pi} dk_x \partial_x \varphi_{k_x,0} = 2 \int_0^\pi \partial_x \varphi_{k_x,0} = 2(\varphi_{\pi,0} - \varphi_{0,0}) \quad (\text{B8})$$

Since we also have $\varphi_{\pi,0}$ and $\varphi_{0,0} = 0 \text{ mod } \pi$ from eq.(B7), the allowed change of $\Phi(k_y = 0)$ in the gauge transformations that preserves the gauge choice eq.(B1) can only be

$$\begin{aligned} \Phi(k_y = 0) &\rightarrow \Phi(k_y = 0) + 4N(\varphi_{\pi,0} - \varphi_{0,0}) \\ &= \Phi(k_y = 0) + 4\pi n, \quad n \in \mathbb{Z} \end{aligned} \quad (\text{B9})$$

The same is true for $\Phi(k_y = \pi)$. Consequently, $\Phi(k_y = 0)$ and $\Phi(k_y = \pi)$ are well-defined modular 4π , so that the Z_2 quantity Δ defined by eq.(B4) is well-defined.

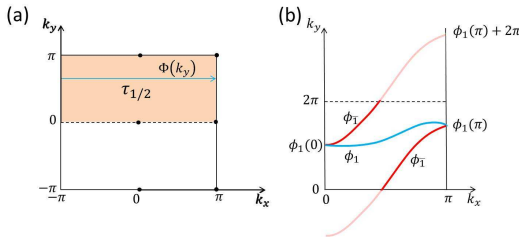


Figure 8: (a) Definition of the half BZ and the paths to define Wilson loops. (b) Schematic picture of eigenvalues $\phi_n(k_y)$ for a two band model. $\phi_1(k_y)$ has winding number 0 and $\phi_{\bar{1}}(k_y)$ has winding number 1, when $\phi_1(0)$ and $\phi_{\bar{1}}(\pi)$ are chosen to be in $[0, 2\pi)$.

Now we relate this result to the non-Abelian Wilson loop. When there are $2N$ bands occupied, a $U(2N)$ Berry phase gauge field $A_i^{nm} = i\langle nk|\partial_i|mk\rangle$ is defined. We can define the $U(2N)$ Wilson loop along the same equal- k_y loops:

$$W(k_y) = P e^{-i\oint dk_x A_x(k_x, k_y)} \in U(2N) \quad (\text{B10})$$

The $U(1)$ gauge field is related to the $U(2N)$ gauge field by $a_i = \text{Tr}A_i$ so that the $U(1)$ flux $\Phi(k_y)$ is related to $W(k_y)$ as $e^{-i\Phi(k_y)} = \det W(k_y)$. Denote the eigenvalues of $W(k_y)$ as $e^{i\phi_n(k_y)}$ with $n = 1, \dots, 2N$, we have $\Phi(k_y) = \sum_n \phi_n(k_y) \text{ mod } 2\pi$. Thus

$$\Delta = \frac{1}{2\pi} \left(\sum_n \int_0^\pi dk_y \partial_{k_y} \phi_n(k_y) - \sum_n (\phi_n(\pi) - \phi_n(0)) \right) \text{ mod } 2 \quad (\text{B11})$$

Now we study the effect of the gauge choice eq.(B1) on the $U(2N)$ gauge field.

$$\begin{aligned} \mathbf{A}_{-\mathbf{k}}^{nm} &= i\langle n, -\mathbf{k}|\nabla_{-\mathbf{k}}|m, -\mathbf{k}\rangle \\ &= -i\mathcal{T}_{ml}\mathcal{T}_{np}T(\langle p\mathbf{k}|\nabla_{\mathbf{k}}|l\mathbf{k}\rangle) \\ &= \mathcal{T}_{ml}\mathcal{T}_{np}(\mathbf{A}_{\mathbf{k}}^{pl})^* = (\mathcal{T}\mathbf{A}_{\mathbf{k}}^T\mathcal{T}^{-1})_{nm} \end{aligned} \quad (\text{B12})$$

$$\Rightarrow W(-k_y) = \mathcal{T}W^T(k_y)\mathcal{T}^{-1} \quad (\text{B13})$$

Thus for $k_y = 0$ or π , $e^{i\phi_n(k_y)}$ is doubly degenerate. If we label a pair of degenerate eigenvalues by n and \bar{n} , the gauge choice eq.(B1) corresponds to the choice of $\phi_n(k_y) = \phi_{\bar{n}}(k_y)$. Indeed we see that if we make this choice, an ambiguity of 2π in ϕ_n leads to an ambiguity of 4π in $\sum_n \phi_n$. Thus Δ defined in eq.(B11) is well-defined. To simplify the formula, we choose $\phi_n(0)$ and $\phi_n(\pi)$ to be in $[0, 2\pi)$. Thus

$$\int_0^\pi dk_y \partial_{k_y} \phi_n(k_y) = \phi_n(\pi) - \phi_n(0) + 2\pi M_n \quad (\text{B14})$$

with M_n the winding number of phase ϕ_n , which is equal to the number of times ϕ_n crosses the line $\phi_n = 2\pi$ from below. For example in Fig.8 (b) ϕ_1 has winding number 0 and $\phi_{\bar{1}}$ has winding number 1. In this way we get

$$\Delta = \sum_n M_n \text{ mod } 2 \quad (\text{B15})$$

The number $\sum_n M_n$ simply counts how many eigenvalues ϕ_n crosses $\phi = 2\pi$ line (or any other reference line) from below. Thus the Z_2 invariant is simply determined by the parity of the number of eigenvalue curves $\phi_n(k_y)$ which crosses a reference line $\phi = \text{constant}$.

-
- ¹ R. B. Laughlin, Phys. Rev. B **23**, 5632 (1981).
- ² D. J. Thouless, M. Kohmoto, M. P. Nightingale, and M. den Nijs, Phys. Rev. Lett. **49**, 405 (1982).
- ³ C. L. Kane and E. J. Mele, Phys. Rev. Lett. **95**, 226801 (2005).
- ⁴ C. L. Kane and E. J. Mele, Phys. Rev. Lett. **95**, 146802 (2005).
- ⁵ J. E. Moore and L. Balents, Phys. Rev. B **75**, 121306 (2007).
- ⁶ R. Roy, Phys. Rev. B **79**, 195322 (2009).
- ⁷ L. Fu and C. L. Kane, Phys. Rev. B **74**, 195312 (2006).
- ⁸ B. A. Bernevig and S. Zhang, Phys. Rev. Lett. **96**, 106802 (2006).
- ⁹ C. Wu, B. A. Bernevig, and S. Zhang, Phys. Rev. Lett. **96**, 106401 (2006).
- ¹⁰ C. Xu and J. E. Moore, Phys. Rev. B **73**, 045322 (2006).
- ¹¹ A. Roth, C. Brune, H. Buhmann, L. W. Molenkamp, J. Maciejko, X. Qi, and S. Zhang, Science **325**, 294 (2009).
- ¹² M. König, S. Wiedmann, C. Brune, A. Roth, H. Buhmann, L. W. Molenkamp, X. Qi, and S. Zhang, Science **318**, 766 (2007).
- ¹³ B. A. Bernevig, T. L. Hughes, and S. Zhang, Science **314**, 1757 (2006).
- ¹⁴ X. Qi, Y. Wu, and S. Zhang, Phys. Rev. B **74**, 085308 (2006).
- ¹⁵ L. Fu, C. L. Kane, and E. J. Mele, Phys. Rev. Lett. **98**, 106803 (2007).
- ¹⁶ L. Fu and C. L. Kane, Phys. Rev. B **76**, 045302 (2007).
- ¹⁷ J. C. Y. Teo, L. Fu, and C. L. Kane, Phys. Rev. B **78**, 045426 (2008).
- ¹⁸ T. Fukui and Y. Hatsugai, J. Phys. Soc. Jpn. **76**, 053702 (2007).
- ¹⁹ Y. Ran, Y. Zhang, and A. Vishwanath, Nature Phys. **5**, 298 (2009).
- ²⁰ H. Zhang, C. Liu, X. Qi, X. Dai, Z. Fang, and S. Zhang, Nat Phys **5**, 438 (2009).
- ²¹ Y. L. Chen, J. G. Analytis, J. Chu, Z. K. Liu, S. Mo, X. L. Qi, H. J. Zhang, D. H. Lu, X. Dai, Z. Fang, et al., Science **325**, 178 (2009), ISSN 0036-8075.
- ²² D. Hsieh, D. Qian, L. Wray, Y. Xia, Y. S. Hor, R. J. Cava, and M. Z. Hasan, Nature **452**, 970 (2008).
- ²³ Y. Xia, D. Qian, D. Hsieh, L. Wray, A. Pal, H. Lin, A. Bansil, D. Grauer, Y. S. Hor, R. J. Cava, et al., Nat Phys **5**, 398 (2009).
- ²⁴ J. G. Analytis, J. Chu, Y. Chen, F. Corredor, R. D. McDonald, Z. X. Shen, and I. R. Fisher, Phys. Rev. B **81**, 205407 (2010).
- ²⁵ D. Hsieh, Y. Xia, D. Qian, L. Wray, F. Meier, J. H. Dil, J. Osterwalder, L. Patthey, A. V. Fedorov, H. Lin, et al., Phys. Rev. Lett. **103**, 146401 (2009).
- ²⁶ S. R. Park, W. S. Jung, C. Kim, D. J. Song, C. Kim, S. Kimura, K. D. Lee, and N. Hur, Phys. Rev. B **81**, 041405 (2010).
- ²⁷ S. Shen, e-print arXiv:0909.4125 (2009).
- ²⁸ B. Yan, C. Liu, H. Zhang, C. Yam, X. Qi, T. Frauenheim, and S. Zhang, EPL (Europhysics Letters) **90**, 37002 (2010).
- ²⁹ H. Lin, L. A. Wray, Y. Xia, S. Xu, S. Jia, R. J. Cava, A. Bansil, and M. Z. Hasan, Nat Mater **9**, 546 (2010).
- ³⁰ M. Z. Hasan and C. L. Kane, e-print arXiv:1002.3895 (2010).
- ³¹ W. Shan, H. Lu, and S. Shen, New J. Phys. **12**, 043048 (2010).
- ³² P. Roushan, J. Seo, C. V. Parker, Y. S. Hor, D. Hsieh, D. Qian, A. Richardella, M. Z. Hasan, R. J. Cava, and A. Yazdani, Nature **460**, 1106 (2009).
- ³³ Z. Alpichshev, J. G. Analytis, J. H. Chu, I. R. Fisher, and A. Kapitulnik, e-print arXiv:1003.2233 (2010).
- ³⁴ W. Lee, C. Wu, D. P. Arovas, and S. Zhang, Phys. Rev. B **80**, 245439 (2009).
- ³⁵ Y. Zhang, K. He, C. Chang, C. Song, L. Wang, X. Chen, J. Jia, Z. Fang, X. Dai, W. Shan, et al., Nat Phys **6**, 584 (2010).
- ³⁶ T. Zhang, P. Cheng, X. Chen, J. Jia, X. Ma, K. He, L. Wang, H. Zhang, X. Dai, Z. Fang, et al., Phys. Rev. Lett. **103**, 266803 (2009).
- ³⁷ X. Zhou, C. Fang, W. Tsai, and J. Hu, Phys. Rev. B **80**, 245317 (2009).
- ³⁸ H. Guo and M. Franz, Phys. Rev. B **81**, 041102 (2010).
- ³⁹ D. Hsieh, Y. Xia, D. Qian, L. Wray, J. H. Dil, F. Meier, J. Osterwalder, L. Patthey, J. G. Checkelsky, N. P. Ong, et al., Nature **460**, 1101 (2009).
- ⁴⁰ D. Hsieh, Y. Xia, L. Wray, D. Qian, A. Pal, J. H. Dil, J. Osterwalder, F. Meier, G. Bihlmayer, C. L. Kane, et al., Science **323**, 919 (2009).
- ⁴¹ T. Fukui, Y. Hatsugai, and H. Suzuki, J. Phys. Soc. Jpn. **74**, 1674 (2005).
- ⁴² D. Xiao, Y. Yao, W. Feng, J. Wen, W. Zhu, X. Chen, G. M. Stocks, and Z. Zhang, Physical Review Letters **105**, 096404 (2010).
- ⁴³ R. D. King-Smith and D. Vanderbilt, Phys. Rev. B **47**, 1651 (1993).
- ⁴⁴ D. J. Thouless, Phys. Rev. B **27**, 6083 (1983).
- ⁴⁵ S. Kivelson, Phys. Rev. B **26**, 4269 (1982).
- ⁴⁶ X. Dai, T. L. Hughes, X. Qi, Z. Fang, and S. Zhang, Phys. Rev. B **77**, 125319 (2008).
- ⁴⁷ A. Kobayashi, O. F. Sankey, and J. D. Dow, Phys. Rev. B **25**, 6367 (1982).
- ⁴⁸ C. Liu, H. Zhang, B. Yan, X. Qi, T. Frauenheim, X. Dai, Z. Fang, and S. Zhang, Phys. Rev. B **81**, 041307 (2010).
- ⁴⁹ W. Zhang, R. Yu, H. Zhang, X. Dai, and Z. Fang, New Journal of Physics **12**, 065013 (2010), ISSN 1367-2630.
- ⁵⁰ S. Murakami, Phys. Rev. Lett. **97**, 236805 (2006).
- ⁵¹ Y. Liu and R. E. Allen, Phys. Rev. B **52**, 1566 (1995).
- ⁵² A. A. Soluyanov and D. Vanderbilt, e-print arXiv:1009.1415 (2010).
- ⁵³ Z. Ringel and Y. E. Kraus, e-print arXiv:1010.5357 (2010).